Polymer 50 (2009) 6057–6064

Contents lists available at ScienceDirect

Polymer

journal homepage: www.elsevier.com/locate/polymer

Highly efficient polymer blends from a polyfluorene derivative and PVK for LEDs

Bruno Nowacki [a], Eduardo Iamazaki [b], Ali Cirpan [c], Frank Karasz [c], Teresa D.Z. Atvars [b], Leni Akcelrud [a,*]

[a] Laboratório de Polímeros Paulo Scarpa (LaPPS) UFPR, Universidade Federal do Paraná, P.O. Box 19081, Curitiba 81531-990, Paraná, Brazil
[b] Instituto de Química, Universidade Estadual de Campinas, P.O. Box 6154, Campinas 13084-971, São Paulo, Brazil
[c] Department of Polymer Science and Engineering, University of Massachusetts at Amherst, MA, USA

ARTICLE INFO

Article history:
Received 16 September 2009
Accepted 19 September 2009
Available online 8 October 2009

Keywords:
Photoluminescence
Electroluminescence
Polymer blends

ABSTRACT

The photophysical and electroluminescent properties of blends of a polyfluorene derivative of the PPV type, poly[(9,9-dihexyl-9H-fluorene-2,7-diyl)-1,2-ethenediyl-1,4-phenylene-1,2-ethenediyl] (labeled as LaPPS16) and poly(vinylcarbazole) – PVK are presented and discussed in terms of the operating light emission mechanisms. Static and dynamic fluorescence measurements and morphology data showed a powerful exciton migration from the host (PVK) to the guest (LaPPS16) resulting in emission coming from solely LaPPS16, even when in concentrations small as 1%. Electroluminescence was greatly enhanced with the blending; increases of 18 times in efficiency and 20 times in luminance were achieved in the blend containing 20% LaPPS16, with 3 V applied voltage.

1. Introduction

Polydialkylfluorenes and related copolymers have been widely investigated for optical–electronic applications because of their high chemical and thermal stability as well as exceptionally high fluorescence quantum yields (0.6–0.8) [1]. The alkyl side chains at the C9 position on the fluorene unit make the polymer solution processable without changing optical and electrical properties [2] by controlling the intermolecular interactions without significantly increasing the steric hindrance in the polymer backbone. Polyfluorenes generally show a low energy emission band in the 500–600 nm range, in addition to the main emission in the solid state, regardless the bulky substitution at the C9 position. The origin of the low energy emission band has been usually attributed to aggregate and/or excimer formation [3]. In the non-substituted polyfluorenes the band can originate from oxidation reactions resulting in the formation of fluorenone in some of the units at the C9 position [4]. The aggregation of conjugated polymers either in the electronic ground state or as excimers is a very common finding, due to the strong tendency of π stacking of the aromatic units. They play an important role because the aggregation quenching of the excited state is one of the main barriers to high luminescence quantum yield [5,6]. The aggregation is characterized by delocalization of the electronic wave function among two or three chains in both the ground and excited states [7]. This results in a broadening of the spectra and reduced color purity. To circumvent this problem several strategies have been employed [8], one of the most efficient is the blending of two light emitting polymers with different band gaps. The enhancement in efficiency that can be achieved is based on three main factors. *First*, exciton–exciton annihilation is substantially lowered or even suppressed due the dilution effect, reducing the degrees of interchain ordering. *Second*, the dipole–dipole interaction between two different chromophores induces a Förster type non-radiative transfer of the excitation energy from a donor to an acceptor. According to the Förster concept, the excitons formed on absorption of higher energy photons at donor sites transfer the energy to acceptor molecules, reducing the degree of exciton quenching, enhancing the PL and EL efficiency [9]. The efficiency of the process is closely related to the spectral overlap between the donor emission and the acceptor absorption. However, it was found that several hosts in the same matrix did not show a direct correlation with the Förster radius [10]. An appropriate description of the overall energy transfer process has to take into account the influence of the acceptor life time on the energy transfer efficiency, in addition to spectral overlap. *Third*, the charge carriers are readily trapped by the acceptor promoting recombination of both electrons and holes. Apart from the enhancement in efficiency, an important aspect of the blending of two EL polymers is the possibility of tuning the optical properties.

Due to its electro- and photo-properties, poly(vinyl-carbazole) (PVK), has been used in various technological applications [11,12]. Polymers based on this compound have been used to enhance LED emission and also for color tuning. In a study of EL of dye doped

* Corresponding author.
E-mail address: leni@leniak.net (L. Akcelrud).

0032-3861/$ – see front matter © 2009 Elsevier Ltd. All rights reserved.
doi:10.1016/j.polymer.2009.09.056

PVK systems [13,14], the hole transport properties of this polymer were demonstrated. Devices in which the emitting layer was formed by PVK blended with other polymeric systems have shown remarkable increases in luminescence efficiency, compared to those in which PVK was not incorporated. As examples one can cite blends of PVK as a matrix for a blue emitting copolyester containing isolated 1,2-dinaphthylene units [10], for poly(3-octyl thiophene) [15,16], and for PPV derivative with silane spacers [17], among others [8]. Other important reasons for the employment of PVK as a host are its favorable film-forming properties, durability at higher temperatures and hole mobility around 10^{-5} cm^2/Vs. In a recent communication we have also discussed the blending strategy for optimization of device performance by blending MEH-PPV with (styrene-*co*-acrylic acid) ionomer [18].

In the present study we show that PVK as a host for a PPV type copolymer poly[(9,9-dihexyl-9H-fluorene-2,7-diyl)-1,2-ethenediyl-1,4-phenylene-1,2-ethenediyl] (LaPPS16) (Fig. 1) has the capability to greatly enhance the EL emission properties of the copolymer, acting both as a energy transfer molecule and a de-aggregating agent. The copolymer, as usually occurs with highly conjugated systems, has a strong tendency to form π stacking aggregates, which redshifts the emission, and is less luminescent and act as traps for the higher energetic isolated chromophores. We chose PVK as a donor polymer because it has a higher energy band gap (ca 3.4 eV) with a strong blue emitting singlet excited-state, peaking around 420 nm [10], spectrally well overlapped with the absorbance of LaPPS16 (ca. 2.56 eV) [19]. Its HOMO level, about −5.8 eV [20] is between those of PEDOT/PSS (ca. 5.0 eV) [21] and LaPPS16. The corresponding band diagram is shown in Fig. 1.

2. Experimental

2.1. Materials

Fluorene (Acros, 98%),hexyl bromide (Aldrich, 98%), paraformaldehyde (Acros, 96%), triphenyl phosphine (Vetec, P.A.), potassium *t*-butoxide (Acros, P.A.), bromidric acid solution in acetic acid (Acros, 33%), methylene chloride (Vetec, P.A.), ethyl ether (Vetec, P.A.), ethanol (Synth, 99,5%), methanol (Vetec, P.A.), chloroform (Vetec, P.A.), and *n*-hexane (Vetec, P.A.), were treated according the literature [22]. The deuterated chloroform used as internal standard for the NMR analyses was Sigma–Aldrich, P.A., containing 1% (V/V) TMS. Chromatographic plates used to follow the dialkylation of fluorene by TLC with dimensions of 2 × 7 cm, were prepared with silica gel 60 (Sigma–Aldrich). In the purifications using a medium pressure chromatographic column, silica from Merck 230–400 mesh was used.

2.2. Chemical procedures

The preparation of poly[(9,9-dihexyl-9H-fluorene-2,7-diyl)-1,2-ethenediyl-1,4-phenylene-1,2-ethenediyl] (LaPPS16) (compound 6 in Scheme 1) followed the Wittig route as described in Scheme 1.

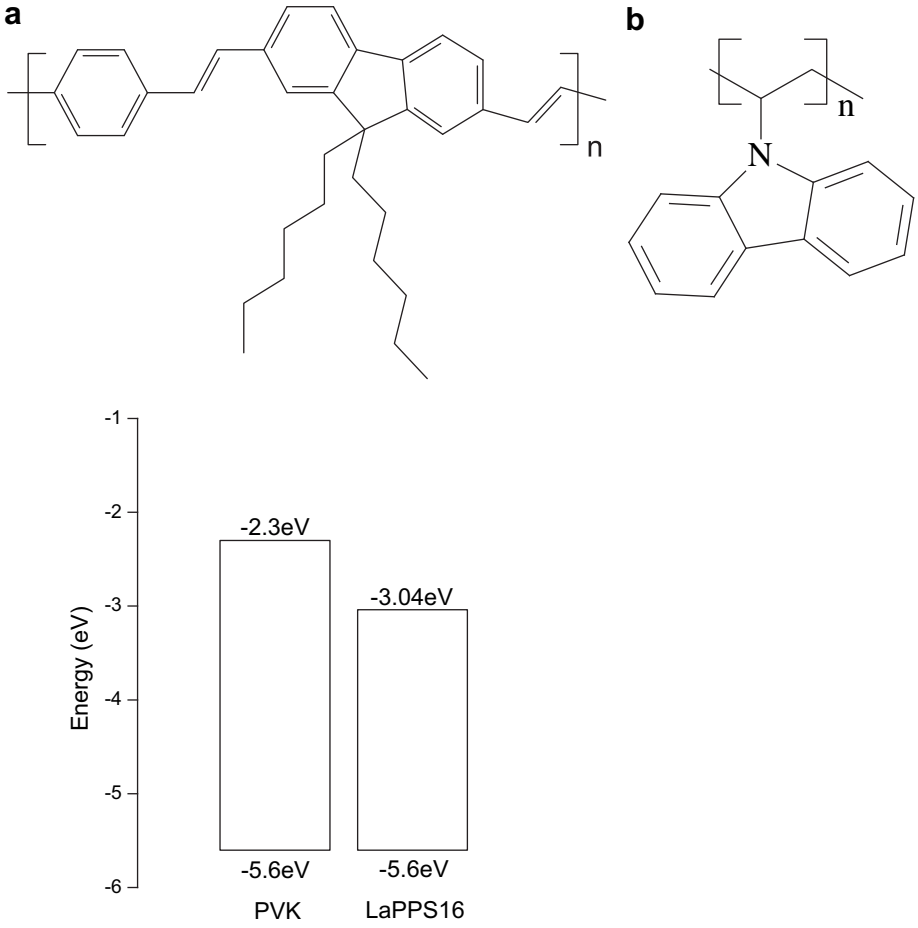

Fig. 1. Chemical structures of polymers poly[(9,9-dihexyl-9H-fluorene-2,7-diyl)-1,2-ethenediyl-1,4-phenylene-1,2-ethenediyl] (LaPPS 16)(a) and poly(vinylcarbazole) (PVK) (b); band diagram of their LUMO and HOMO levels.

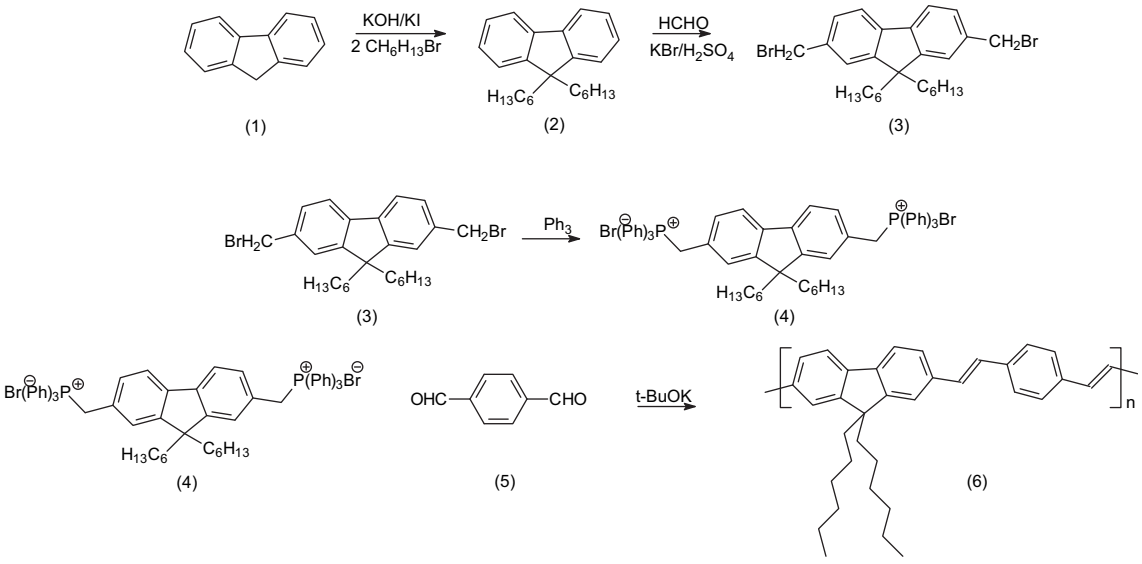

Scheme 1. Chemical route for the synthesis of poly[(9,9-dihexyl-9H-fluorene-2,7-diyl)-1,2-ethenediyl-1,4-phenylene-1,2-ethenediyl] (LaPPS16).

2.3. Synthesis of 9,9 di-n-hexylfluorene (compound **2** in Scheme 1) [23]

To a mixture containing fluorene [17.01 g (0.1 mol)] (**1**); KOH in powder form [28.02 g (0.5 mol)] and KI 0.08 g (0.0005 mol) in 45 mL DMSO, 39 mL (46.17 g) hexyl bromide were added drop wise during 90 min. The mixture was kept overnight with stirring at 25 °C, and then diluted with water (600 mL). The organic phase was extracted with toluene (3 × 100 mL) and the solvent removed by evaporation. A purple colored oil was obtained, which after distillation at 230 °C under 6–10 mmHg yielded 30.06 g of a yellow oil. Yield = 88%. The product was purified by column chromatography using hexane as solvent, which was further removed by evaporation, and a colorless oil was collected. ^{1}H NMR($CDCl_3$) δ7.68 (m, 2H), 7.30 (m, 6H), 1.95 (m, 4H), 0.93–1.19 (m, 12H), 0.75 (t, 6H), 0.60 (m, 4H).

2.4. Synthesis of 2,7-bis(bromomethyl)-9,9′-di-n-hexylfluorene (compound **3** in Scheme 1) [22]

To a mixture of 12.0 g (35.9 mmol) of 9,9′–di-*n*-hexylfluorene, 12.28 g (391 mmol) of paraformaldehyde; 53.16 g (0.45 mol) potassium bromide and 90 mL of glacial acetic acid, a mixture of 41 mL acetic acid and 41 mL sulphuric acid was added drop wise. The reaction medium was kept at 60 °C, with stirring for 20 h, and then poured onto 500 mL of a distilled water/ice mixture. The organic phase was extracted with methylene chloride (3 × 200 mL). The fractions were collected and washed with a saturated sodium chloride aqueous solution. The solvent was removed under reduced pressure yielding 17.01 g of a yellow oil. Yield = 91%. ^{13}C NMR ($CDCl_3$) δ151.65, 140.73, 136.88, 127.98, 123.65, 120.02, 55.12, 40.06, 34.40, 31.34, 29.52, 23.63, 22.45, 13.96.

2.5. Synthesis of 2,7-bis[(p-triphenyl phosphonium)methyl]-9,9′-di-n-hexylfluorene dibromide (compound **4** in Scheme 1) [23]

A mixture of triphenyl phosphine [12,59 g, (48 mmol)]; 2,7-bis(bromomethyl)-9,9′-di-n-hexylfluorene [8.23 g, (15,84 mmol)] and dimethylformamide (95 mL) was maintained under reflux for 12 h. It was then cooled to room temperature and slowly added to 450 mL ether with constant stirring. The white precipitate obtained was filtered, washed with ether and dried under vacuum at 40 °C, resulting in 15.98 g of product. Yield = 96.8%. ^{13}C NMR ($CDCl_3$) δ150.97, 140.09, 134.83, 134.04, 133.84, 129.99, 129.74, 125.70, 118.11, 116.41, 54.57, 39.53, 31.31, 29.22, 29.02, 23.50, 22.28, 13.72.

2.6. Synthesis of poly[(9,9-dihexyl-9H-fluorene-2,7-diyl)-1,2-ethenediyl-1,4-phenylene-1,2-ethenediyl] (LaPPS16) [23]

2.0612 g (1.97 mmol) of 2,7-bis[(p-triphenylphosphonium)-methyl]-9,9′-di-n-hexylfluorene dibromide and 0.2701 g (1.97 mmol) of terephthaldhyde were dissolved in 20 mL chloroform. 20 mL of an ethanol solution of potassium *t*-butoxide 1.1071 g (9.87 mmol, 2.5 eqv.) were added drop wise at room temperature. After reacting overnight 5 mL of hydrochloric (2% w/v) acid were added slowly, and the mixture was poured over 800 mL cold methanol with stirring. After filtration, the collected yellow precipitate was dissolved in 10 mL chloroform and re-precipitated in 800 mL cold methanol. The polymer was filtered and dried under vacuum for 48 h, resulting in 0.59 g of product. Yield = 65%. FTIR spectra show two maxima at 960 and 823 cm^{-1}, representing -trans and -cis conformations respectively of the vinylic bond formed on the Wittig reaction. Integrating aliphatic and aromatic peaks of ^{1}H NMR spectrum, we obtained a ratio 0.573 for 14H aromatic and 26 aliphatic hydrogens.

The T_g was 123 °C, as measured by DSC and M_w = 9665.as measured by GPC.

2.7. Blend preparation

The blends were prepared by co-precipitation of the polymers from mixed solutions in chloroform. Each component was diluted to 10^{-3} mol/L and the appropriate amounts were mixed and precipitated with methanol. The blend composition varied from 1%, to 20% of LaPPS16 in the PVK matrix, on a molar basis, dividing the sample weight by the mol of the repeating unit of the corresponding polymer.

2.8. Characterization

FTIR spectra were taken of KBr pellets using a BIORAD FTS 3500 GX spectrometer, in the 400–4000 cm^{-1}, range, in the transmittance mode. The UV–Vis spectra were taken in a Shimadzu spectrophotometer model NIR 3101.

The molar masses of the copolymers were measured by a gel permeation chromatograph Agilent 1100 equipped with

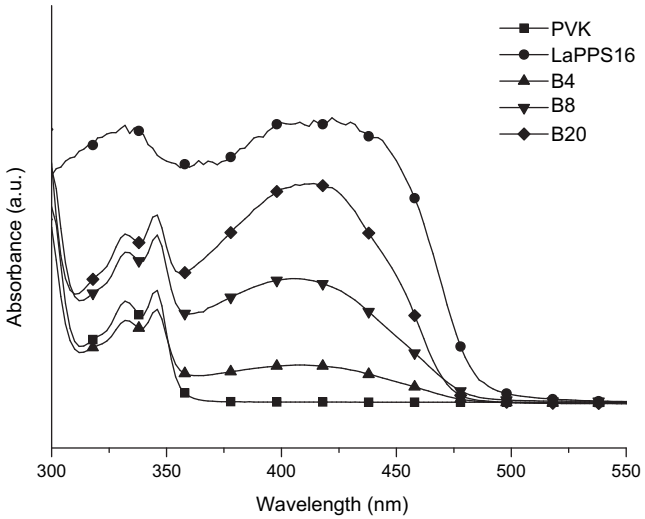

Fig. 2. Electronic absorption spectra of the PVK, LaPPS16 and their mixtures (B4% = 4%, B8 = 8%, B20 = 20% of LaPPS16) in chloroform solution (10^{-4} mol/L).

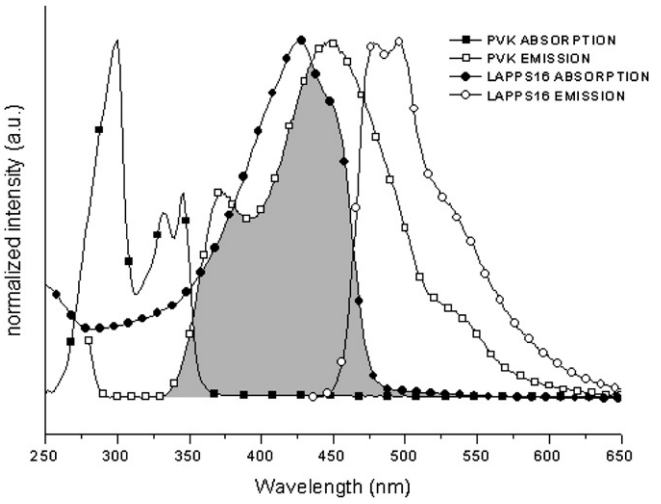

Fig. 4. Normalized electronic absorption and fluorescence emission spectra of PVK ($\lambda_{exc} = 294$ nm) and LaPPS16 ($\lambda_{exc} = 340$ nm) in chloroform solutions. The shaded region corresponds to the spectral overlap between the two components.

a refractive index detector and PL gel mixed C and B columns in series, at 35 °C, using DMF as solvent and monodisperse polystyrene samples as standards.

NMR ^{1}H and ^{13}C analyses were performed using a Brucker 200 MHz Advance spectrometer using solutions of chloroform-d with TMS as internal standard.

Steady-state fluorescence spectroscopy was performed in a UV 2401 PC Shimadzu spectrophotomer, double beam. For solutions a square cuvette of 1 cm was used. Films were supported on glass slides and the emission spectra were recorded using a front-face sample orientation. For PVK the emission spectral range was from 300 nm to 525 nm with an excitation wavelength of 264 nm and for LaPPS16 and its blends the emission spectral range was from 380 nm to 650 nm using an excitation wavelength of 340 nm. Slits were selected for a spectral resolution of ±1 nm in excitation and in emission.

Fluorescence decays were recorded in a Single Photon Counting Edinburgh Analytical nF900 system using a pulsed hydrogen lamp with frequency rate of 40 kHz. Solid state samples were maintained in a sealed quartz cuvette under vacuum and a degassed quartz cuvette was used for solutions. Decay curves were determined using $\lambda_{exc} = 300$ nm and $\lambda_{em} = 410$ nm for PVK chloroform solutions, for LaPPS16 films and LaPPS16/PVK blends. For LaPPS16 and LaPPS16/PVK chloroform solutions we used $\lambda_{exc} = 340$ nm and $\lambda_{em} = 475$ nm because of the lack of emission at 410 nm. The observed emission decays $R(t)$ is determined by the pulse intensity distribution $G(t)$ (determined using a Ludox® scattering solution) and the total response $F(t)$. The data were analyzed using a multi-exponential decay function where the pre-exponent B_i represents the fractional contribution of each specific lifetime τ_I (equation (1)). The theoretical multi-exponential function fits the experimental curve using a Marquardt algorithm and the software purchased from Edinburgh. Good fits were obtained when the χ^2 is approximately 1.

$$F(t) = \sum_{i=1}^{N} B_i \exp[-t/\tau_i] \quad (1)$$

where B_i is a pre-exponential factor representing the fractional contribution to the time-resolved decay of the component with a lifetime τ_i and t is the time.

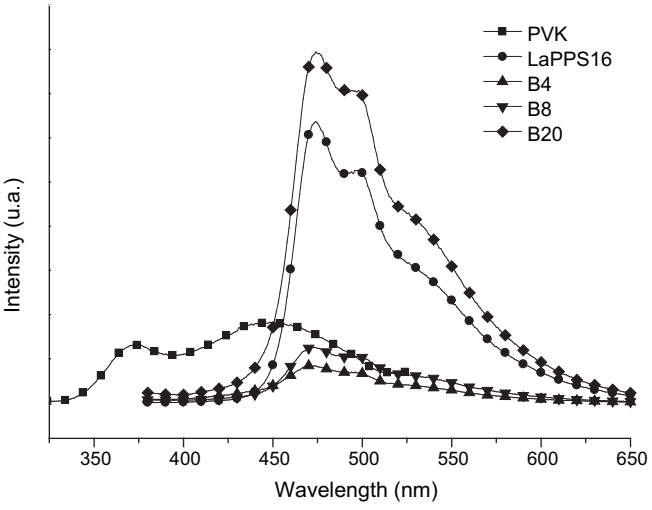

Fig. 3. Emission spectra of PVK ($\lambda_{exc} = 294$ nm), LaPPS16 ($\lambda_{exc} = 340$ nm) and their mixtures (B4% = 4%, B8 = 8%, B20 = 20% of LaPPS16) ($\lambda_{exc} = 340$ nm) in chloroform solution (10^{-4} mol/L).

Table 1
(a) Fluorescence lifetimes (t_1, t_2), % population of emitting species (B) of PVK, LaPPS16 and their mixtures in chloroform solutions (10^{-4} mol L^{-1}) and films. (b) Life times of the pure polymers and the blends in film form. c^2 is a fitting parameter which best value is close to one and the residual distribution is random.

(a)					
Solutions (λ_{em})	τ_{F1} (ns)	B_1	τ_{F2} (ns)	B_2	χ^2
PVK (410 nm)	1.50 ± 0.01	0.63	6.64 ± 0.01	0.37	1.176
LAPPS16 (475 nm)	1.02 ± 0.01	0.85			1.238
B2 (475 nm)	0.99 ± 0.02	0.79			1.101
B8 (475 nm)	1.06 ± 0.06	0.91			1.182
B20 (475 nm)	0.99 ± 0.02	0.82			1.076
(b)					
Films (λ_{em})	τ1 (ns)	*B*1	τ2 (ns)	*B*2	χ^2
PVK (410)	1.65 ± 0.02	0.043	9.62 ± 0.05	0.02	1076
LAPPS16 (410)	0.22 ± 0.01	0.225	2.72 ± 0.02		1291
LAPPS16 (550)	0,45 ± 0.02	0.092	2.36 ± 0.07		1135
B2 (410)	0.22 ± 0.01	0.228	4.14 ± 0.02		1319
B2 (550)	0.55 ± 0.02	0.079	2.56 ± 0.02		0996
B8 (410)	0.20 ± 0.01	0.24	5.56 ± 0.01		1219
B8 (550)	0.66 ± 0.03	0.061	2.54 ± 0.01	0.01	1042
B20 (410)	0.18 ± 0.01	0.28	3.52 ± 0.05		1415
B20 (550)	0.39 ± 0	0.1	2.12 ± 0.01	0.01	1217

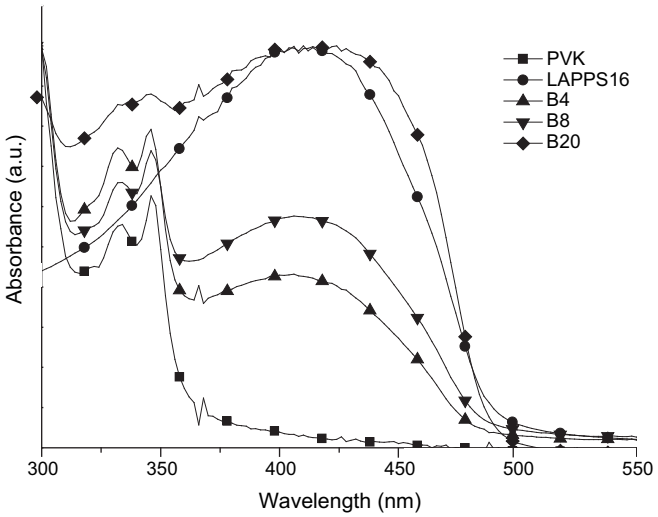

Fig. 5. Absorption spectra of PVK, LaPPS16 and of the blends in the solid state.

Epifluorescence images of every polymer blend was recorded with a microscope Leica DM IRB, employing a mercury arc lamp HBO (HBO-100 W) for excitation using a optical filter for wavelength range of 330–380 nm. The epifluorescence image was separated from the excitation beam by a dichroic mirror selected for $\lambda_{em} > 410$ nm. To improve the contrast a white lamp was combined with the UV excitation beam. Objective magnifications of 50× were used and the images were taken with a Samsung SDC-311 camera processed with the Linksys v. 2.38 software. Blue regions from the images are due to the fluorescence from PVK and bright domains arise from LaPPS16.

Atomic force microscopy (AFM) images were acquired with a SHIMADZU SPM-9500 J3 AFM microscope, using a pyramidal pointer with a silicon nitride square base (2.9 μm × 4 μm), operating em contact mode with a cantilever with spring constant of 0.15 N/m, at a frequency of 24 kHz, and with 200 μm length. The measurements were performed at ambient conditions with variable scan rate. For image treatment the software of the SPM program from Shimadzu was used. The samples were diluted with chloroform, at a concentration of 1 g/10 mL and 1 mL of each solution was spin coated on mica surface at 500 rpm during 10 s. The films were dried in a vacuum oven for 24 h before the measurements.

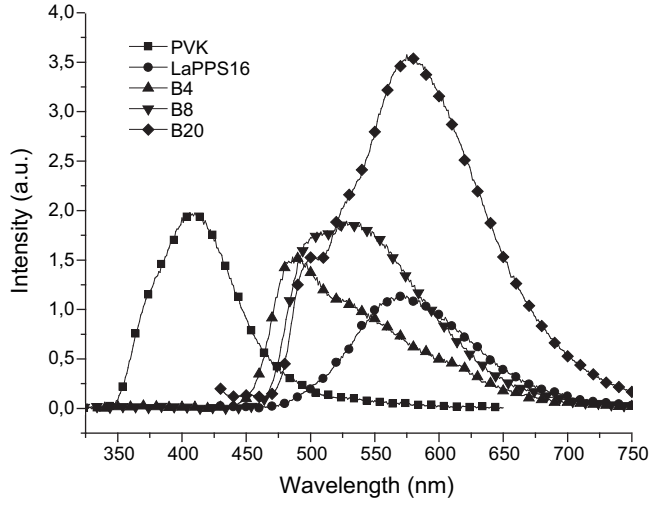

Fig. 6. Emission Spectra of PVK, LaPPS16 and their blends. λ_{exc} (PVK) = 264 nm, λ_{exc} (LaPPS16 and blends) = 426 nm.

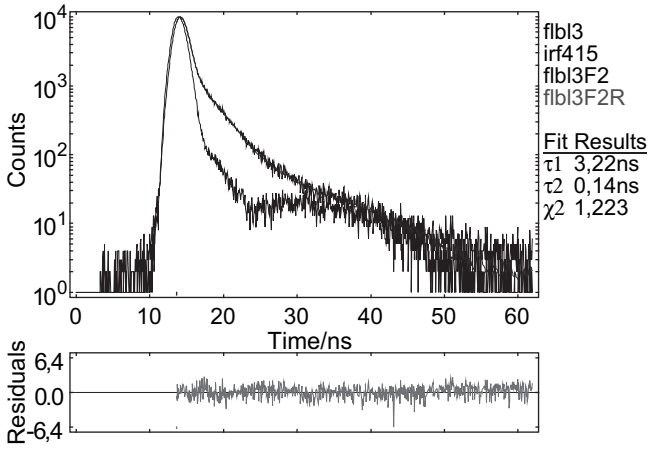

Fig. 7. Decay curve for B20 in film form.

2.9. Device preparation

Poly(3,4-ethylenedioxithiophene)/poly(styrenesulfonate) (PEDOT:PSS) (Bayer Corporation) was deposited by spin-coating onto a glass plate covered with ITO blend (OFC Corporation, 20 ohms sq^{-1}), dried at 100 °C for 1 h under vacuum. A chloroform polymer solution (20 mg mL^{-1}) was filtered and deposited by spin-coating over the PEDOT:PSS layer, under dry nitrogen at 2000 rpm. The polymer films were typically 75 nm thick. A metallic calcium layer (400 nm thickness) was deposited on top of the polymer layer by sublimation at 10^{-7} Torr, followed by a protective layer of aluminum on top. The final configuration of the device was ITO/PEDOT:PSS/polymer layer/Ca/Al.

The devices were characterized using a system described previously [24]. The electroluminescence characterization of the devices was done with an Oriel monochromator and a calibrated photometer International Light Inc., model IL 1400a, under argon.

3. Results and discussion

3.1. Photophysical properties of LaPPS16 in solutions

Fig. 2 displays the electronic absorption bands of PVK, LaPPS16 and mixtures of these two polymers in chloroform solutions in the compositions of 4%, 8% and 20% of LaPPS16. The total concentration

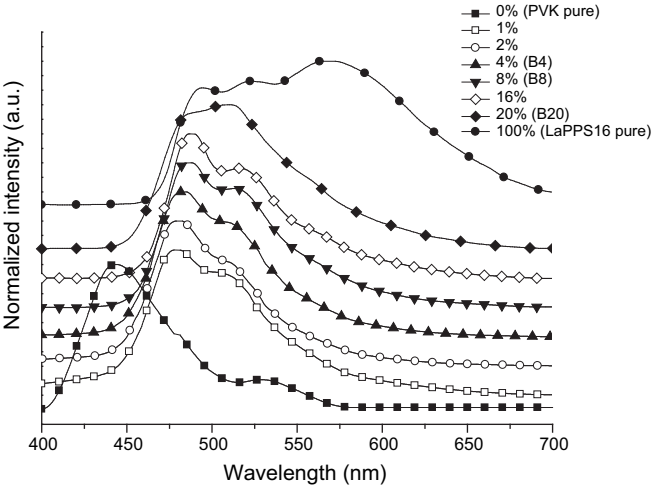

Fig. 8. EL spectra of PVK, LaPPS16 and their blends.

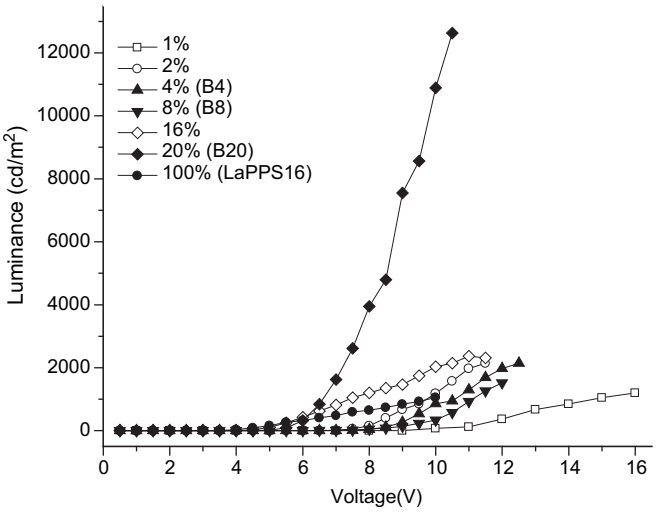

Fig. 9. Voltage vs. luminance of the devices made with PVK and their blends.

was maintained constant and equal to 10^{-4} mol/L, only the relative amount of the components was varied. The PVK lower energy absorption band has a vibronic structure with a maximum at 394 nm. The lower energy characteristic peak of LaPPS16 is broad and centered at 415 nm. Its relative intensity in the solutions containing both polymers is proportional to the concentration of each component in the mixture. In the blue part of the spectra, PVK maintains its profile and increases somewhat due to the contribution of LaPPS16 that also absorbs in this region.

The corresponding emission spectra of these samples in chloroform solution are shown in Fig. 3. The PVK characteristic peaks ($\lambda_{exc} = 294$ nm) were located at $\lambda_{em} = 372$ and 448 nm. Its emission spectrum at room temperature is frequently composed of two overlapped bands: the higher energy is associated with the isolated lumophores and the lower energy is attributed to excimers ($\lambda_{em} \approx 440$ nm). [25–38]. The relative intensity of these two bands depends on the polymer tacticity, the molecular weight, the polymer concentration in solution and on the temperature. The presence of excimeric species (broad emission at 448 nm) indicates that in the concentrations used associated species are formed, generated by inter and intrachain chromophoric interactions.

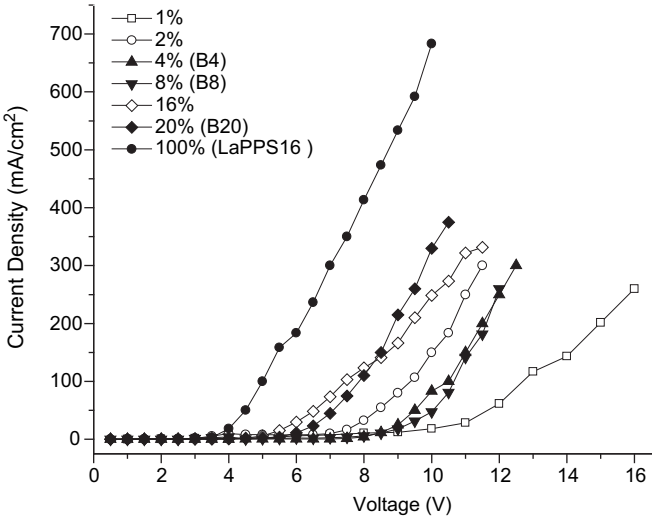

Fig. 10. Currrent density vs. voltage LEDs made with LaPPS16, PVK, and their blends.

Table 2
Data obtained with the LEDs made with LaPPS16, PVK, and their blends. Diode configuration ITO/PEDOT/polymer layer/Ca/Al.

% LaPPS16 in PVK matrix	Turn-on voltage (V)	Luminescence efficiency (cd/A)	Maximum luminance (cd/m^2)
1%	7	0.60	1200 (16 V)
2%	5	0.86	2258 (11.5)
4%	4.5	1.08	2142 (12.5 V)
8%	4	1.20	1522 (12 V)
16%	3	1.70	2311 (11.5 V)
20%	3	3.61	12630 (10.5 V)
100%	3	0.20	1059 (10 V)

The emission spectrum of LaPPS16 ($\lambda_{exc} = 340$ nm) was observed at $\lambda_{em} = 474$ nm with vibronic peaks at 498 and 530 nm. The higher intensity of the red-edge band is an indication of the aggregates in solution. The peak profile is very similar to that observed for other polyfluorenes [39–43].

When both polymers are in the common solvent, the PVK emission was completely suppressed. This quenching was attributed to an energy transfer process from the PVK in the excited state to LaPPS16, due to the strong overlap between the PVK emission and the LaPPS16 absorption as shown in Fig. 4.

Fluorescence decay curves were recorded for chloroform solutions of PVK, LaPPS16 and their mixtures in chloroform solutions at the same compositions at room temperature (curves not shown). Lifetimes are summarized in Table 1. The PVK fluorescence decay was determined using $\lambda_{exc} = 300$ nm and $\lambda_{em} = 410$ nm (where the emission peak is located). This experimental curve can be fitted by a biexponential function with two lifetimes: $\tau_{F1(PVK)} = 1.50 \pm 0.01$ ns ($B_1 = 0.63$) and $\tau_{F2(PVK)} = 6.64 \pm 0.01$ ns ($B_2 = 0.37$). These two decays are faster than the values reported for PVK probably due to the concentration of the solution that induces a dynamic quenching of the electronic excited state [38,44,45].

The LaPPS16 decay was measured using $\lambda_{exc} = 340$ nm and $\lambda_{em} = 475$ nm (where the emission peak is located). The experimental curve could again be fitted by a monoexponential function with a main lifetime of $\tau_{F1(LaPPS16)} = 1.02 \pm 0.01$ ns ($B_1 = 0.85$). Values between 0.2 and 1.0 ns have been typically reported for several polyfluorenes [46,47]. We also observed that under the same excitation and emission wavelengths, the fluorescence lifetime of LaPPS16 is practically constant and independent of the relative amount of PVK (Table 1). Under our experimental conditions the PVK lifetime cannot be determined in the presence of LaPPS16 since it is completely quenched as shown in Fig. 3. Therefore, the quenching mechanism is not discussed here.

3.2. Photophysical properties of LaPPS16 in the solid state

The solid state absorption spectra of PVK, LaPPS16 and their blends containing 4%, 8% and 20% of LaPPS16 in PVK matrix are shown in Fig. 5. The PVK film presented well defined peaks at 294, 335 and 345 nm, the two lower energy peaks represent the vibronic progression of the low lying singlet state. The absorption profile did not present any noticeable difference relative to that of the solution. LaPPS16 absorption was characterized by a broad band peaking at 410 nm. All characteristic absorption bands of the pure components were present in the blends spectra, whose intensity varied according to the content of each one.

The emission profiles of the pure components and of the blends are shown in Fig. 6. The PKV emission spectrum ($\lambda_{exc} = 264$ nm) in the solid state shows a broad band centered at 420 nm, and that of LaPPS16 is centered at 550 nm ($\lambda_{exc} = 340$ nm). For the blends, the emission spectra followed the same trend as in solution. Under excitation $\lambda_{exc} = 264$ nm, no emission from PVK is observed.

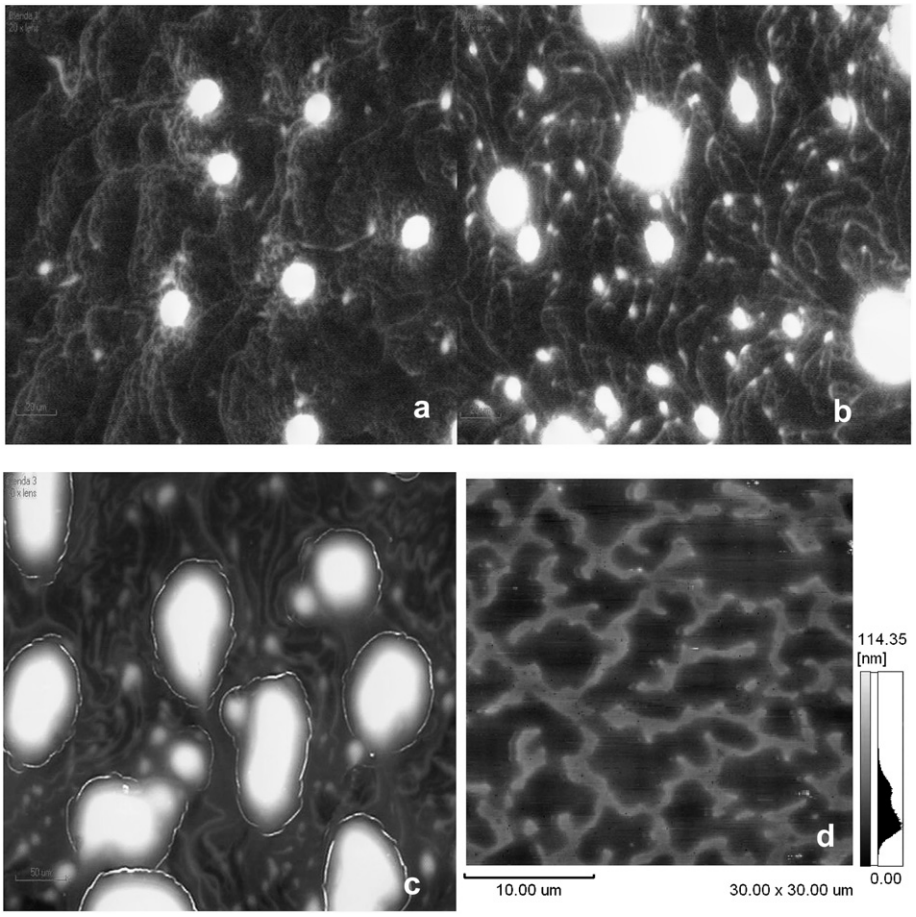

Fig. 11. Epifluorescence images of the blends (a) B4, (b) B8, (c) B20, (d) AFM image of B20.

Therefore, we assume that a complete energy transfer is occurring from the PVK electronic excited state to the LaPPS16 macromolecules. Even in concentrations as small as 1%, LaPPS16 emission is the only one observed.

The results from time resolved emission studies in the solid state are summarized in Table 1. We also observe that the contribution of the emission decay (B_i) to the total signal is always small due to the high light scattering of those films. Nevertheless, the data (emission of the blend in film form) reveals that the contribution of τ_1 at 410 nm is 96–99% in the emission region of LaPPS16. This indicates complete energy transfer of the PVK isolated exciton to the polyfluorene, confirming the results obtained in steady state conditions where complete suppression of the PVK emission took place. In other wavelengths the decay of more complex species is observed, such as those of associated forms from the same species or from different chromophores. Earlier studies revealed the high tendency to aggregation of LaPPS16 [48]. In a general way the decay data clearly demonstrated that apart from other emission mechanisms, the energy transfer from PVK to LaPPS16 is the predominant phenomenon in the studied blends. In Fig. 7 the decay curve of the blend B20 (20% LaPPS16 in PVK) is illustrated.

3.3. Electroluminescence

Fig. 8 presents the EL spectra of the pure components and of the blends. PVK displayed peaks at 443 and 530 nm and LaPPS16 at 492, 519 and 570 nm, significantly redshifted in relation to the PL emission. The differences between EL and PL spectra are attributed to the differences between the optical and electrical excitation mechanisms. In the PL process, the LaPPS16 is only the acceptor in the Förster mechanism. In the EL process it not only plays this role, but also is the carrier-trapping and emitting center. The blends emitted at the same location as LaPPS16 (492 and 519 nm) with a small redshift that increased with progressive increases in LaPPS16 in the blend. The PVK emission was suppressed.

The results of luminance *vs* voltage measurements, presented in Fig. 9 showed that the materials had turn-on voltages in the range 4–6 V. The device made with blend B20, with a turn-on of 5.5 V attains a luminance of 12630 cd/m^2 at 10 V, being the most efficient among all the compositions tested.

In Fig. 10 the curves relating the current density with voltage are displayed. In all samples the current begins to flow in the polymer layer at around 4 V. Nevertheless in pure LaPPS16 the current density is higher than in the blends, attaining 700 mA/cm^2 at 10 V, whereas in the blends 300–400 mA/cm^2 are attained at higher voltages. This result indicates that LaPPS16 has a higher conductivity than PVK.

In the band diagram, shown in Fig. 1 the HOMO and LUMO levels of the LaPPS16 fall within the band gap of PVK indicating that the holes and electrons are readily trapped by LaPPS16. Since the trapping mechanism can effectively promote recombination of both carriers on LaPPS16, the PVK host provides a lower contribution in the EL spectrum than in the PL spectrum.

The results obtained with the diodes are displayed in Table 2

The results for the blend containing 20% LaPPS16 when compared with those of the pure polymer show that an enhancement of 18 times was achieved in EL efficiency and 12 times in luminance. These values were obtained with a low applied voltage,

3 V. The emission intensity of 12630 cd/m^2 is one of the highest found for polyfluorene derivatives.

The collected images in the fluorescence and AFM microscopes are presented in Fig. 11. Epifluorescence images show that in the blend containing 4% LaPPS16, the domains of this polymer are clearly seen, with dimensions around 20 μm which increase in size and size distribution when the concentration is increased to 8%. In the blend with 20% LaPPS16 the formation of an interface is distinctly observed, which could be related to an associated species between the two components, corresponding to the different decay times observed. A percolation path is also perceptible, that would contribute to enhance the charge transport in electroluminescence. AFM image of blend containing 20% LaPPS16 shows the formation of a co-continuous structure. This morphology could account for the observed photophysical and electroluminescent behavior. It also accounts for the fact that the driving voltages of the blends increase with increases in PVK content, supporting the conclusion that the transport of charge carriers is retarded by this component; the apparent resistance increases with larger amounts of PVK in the blends.

4. Conclusions

The static and time resolved fluorescence results with epifluorescence and AFM images demonstrated that the energy transfer from PVK to the fluorene copolymer is the main mechanism responsible for the enhancement of light emission either in PL as in EL, in accordance with the large spectral overlap between the two polymeric species involved.

Acknowledgments

BN, EI, TDZA and LA whish to thank CNPq, FAPESP and CAPES; FEK and AC are grateful to AFORS for financial support.

References

[1] Liu B, Huang W. Thin Solid Films 2002;41(7):206.
[2] Long X, Grell M, Malinovski A, Bradley DDC, Inbasekaran M, Woo EP. Opt Mater 1998;9:70–6.
[3] Gaal M, List JW, Scherf U. Macromolecules 2003;36(12):4236.
[4] List EJW, Guentner R, de Freitas PS, Scherf U. Adv Mater 2002;14:374.
[5] Jakubiak R, Collison CJ, Wan WC, Rothberg LJ, Hsieh BR. J Phys Chem A 1999;103:2394.
[6] Chang R, Hsu JH, Fann WS, Yu J, Lin SH, Lee YZ, et al. Chem Phys Lett 2000;317:153.
[7] Nguyen T-Q, Doan V, Schwartz BJ. J Chem Phys 1999;110:4068.
[8] Akcelrud L. Prog Polym Sci 2003;28:875.
[9] Nishino H, Yu G, Heeger AJ, Chen TA, Rieke RD. Synth Met 1995;68:243.
[10] Yu JW, Kim JK, Kim DY, Kim C, Song NW, Kim D. Curr Appl Phys 2006;6:59.
[11] Nespurek S. Synth Met 1993;61:55.
[12] Zhang C, Von Seggern H, Kraabel B, Schimdt WH, Heeger AJ. Synth Met 1995;72:185–8.
[13] Partridge RH. Polymer 1983;24(6):733–8.
[14] Partridge RH. Polymer 1983;24(6):748–54.
[15] Wang G, Yuan C, Wu H, Wei Y. J Appl Phys 1995;78(4):2679–83.
[16] Mort L, Pfister G. Electronic properties of polymers. New York: Wiley/Interscience; 1982.
[17] Ryu MK, Lee JH, Lee SM, Zyung T, Kim HK. ACS Polym Mater Sci Eng Proc 1996;75(2):408.
[18] Cossielo RF, Cirpan A, Karasz FE, Akcelrud LC, Atvars TDZ. Synth Met 2008;158:219.
[19] Lee TW, Park JH, Park OO, Lee J, Kim JC. Opt Mater 2007;30:486.
[20] Zheng H, Zhang R, Wu F, Tian W, Shen J. Synth Met 1999;100:291.
[21] Fulghum TM, Taranekar P, Advincula RC. Macromolecules 2008;4:5681.
[22] Perrin DD, Armarego WL, Purification of Laboratory Chemicals. 3rd ed. Oxford: Butterworts Heinemann, 1988.
[23] Zheng M, Ding L, Lin Z, Karasz FE. Macromolecules 2002;35:9939.
[24] Ding L, Karasz FE. J Appl Phys 2004;96:2272.
[25] Klopffer W. Chem Phys 1981;57.
[26] Wada Y, Ito S, Yamamoto M. J Phys Chem 1993;97:11164.
[27] Keyanpour-Rad M, Ledwith A, Hallam A, North M, Breton M, Hoyle C, et al. Macromolecules 1978;1:1114.
[28] Ng D, Guillet JE. Macromolecules 1981;14:405.
[29] Somersall AC, Guillet EJ. Macromolecules 1973;6:218.
[30] Sakai H, Itaya A, Masuhara H, Sasaki K, Kawata S. Chem Phys Lett 1993;208.
[31] Skilton PF, Ghiggino KP. Polym Photochem 1984;5:179.
[32] Roberts AJ, Phillips D, Abdul-Rasoul FAM, Ladwith A. J Chem Soc Faraday Trans 1981;77:2725.
[33] Buchberger EM, Mollay B, Weixelbaumer WD, Kauffmann HF. J Chem Phys 1988;89:635.
[34] Johnson GE. J Chem Phys 1975;62:4697.
[35] Sakurovs R, Ghiggino KP. Aust J Chem 1981;34:1367.
[36] Itaya, Sakai H, Masuhara H. Chem Phys Lett 1987;138:231.
[37] Sarkar A, Chakravorti S. J Lumin 1998;78:205.
[38] Martins TD, Weiss RG, Atvars TDZ. J Braz Chem Soc 2008;19(8):1450.
[39] Gruber J, Li RWC, Aguiar LHJMC, Garcia TL, Oliveira HPM, Atvars TDZ, et al. Synth Met 2006;156:104.
[40] Herz LM, Phyllips RT. Phys Rev B 2000;61:13691.
[41] Dias FB, Morgado J, Maçanita AL, Costa PC, Burrows HD, Monkman AP. Macromolecules 2006;39:5854.
[42] Traiphol R, Charoenthai N, Srikhirin T, Kerdcharoen T, Osotchan T, Maturos T. Polymer 2007;48:813.
[43] Oliveira HPM, Martins TD, Honório KM, Rodrigues PC, Akcelrud LC, Silva ABF, et al. J Braz Chem Soc 2009;19:160.
[44] Soutar I, Swanson L, Davidson K, Yin J. High Perform Polym 1997;9:353.
[45] Hejboer J. Polymer 1987;28:509.
[46] Oliveira HPM, Cossiello RF, Atvars TDZ. Quim Nova 2006;29:277.
[47] Palsson LO, Vaughan HL, Monkman AP. J Chem Phys 2006;125:164701.
[48] Tozoni JR, Guimarães FEG, Atvars TDZ, Nowacki B, Akcelrud L, Bonagamba TJ. Eur Polym J 2009;45(8):2467.